Korean J. Chem. Eng., 35(10), 2065-2077 (2018)
DOI: 10.1007/s11814-018-0123-8

pISSN: 0256-1115
eISSN: 1975-7220

Potential of different additives to improve performance of potassium carbonate for CO_2 absorption

Rouzbeh Ramezani*,†, Saeed Mazinani, and Renzo Di Felice***

*Department of Civil, Chemical and Environmental Engineering, University of Genoa, Via Opera Pia 15, 16145 Genova, Italy
**Department of Chemical Engineering, KU Leuven, Celestijnenlaan 200F, B-3001 Leuven, Belgium
(*Received 4 April 2018 • accepted 18 July 2018*)

Abstract−The performance of potassium carbonate (K_2CO_3) solution promoted by three amines, potassium alaninate (K-Ala), potassium serinate (K-Ser) and aminoethylethanolamine (AEEA), in terms of heat of absorption, absorption capacity and rate was studied experimentally. The experiments were performed using a batch reactor, and the results were compared to pure monoethanolamine (MEA) and K_2CO_3 solutions. The heat of absorption of K_2CO_3+additive solution was calculated using the Gibbs-Helmholtz equation. In addition, a correlation for prediction of CO_2 loading was presented. The results indicated that absorption heat, absorption rate and loading capacity of CO_2 increase as the concentration of additive increases. The blend solutions have higher CO_2 loading capacity and absorption rate when compared to pure K_2CO_3. The heat of CO_2 absorption for K_2CO_3+additive solutions was found to be lower than that of the pure MEA. Among the additives, AEEA showed the highest CO_2 absorption capacity and absorption rate with K_2CO_3. In conclusion, the K_2CO_3+AEEA solution with high absorption performance can be a potential solvent to replace the existing amines for CO_2 absorption.

Keywords: Greenhouse Gas, CO_2 Capture, Heat of Absorption, CO_2 Solubility, Absorption Rate

INTRODUCTION

A huge amount of greenhouse gases released through burning of fossil fuels are causing global warming [1]. Carbon dioxide, as one of the most important greenhouse gases due to its abundance in the atmosphere, has a significant effect on global warming [2]. Therefore, it is essential to reduce CO_2 emission to decrease the concentration of greenhouse gasses into the atmosphere. CO_2 capture from power plants can be technically applied by several technologies [3]. Chemical absorption of CO_2 into liquid solvent is the most attractive technology because of its advantages, including its compatibility with the low partial pressure of CO_2 in flue gas and its applicability to the current operating facilities [4]. An ideal solvent should have several desired parameters, including fast kinetic, high CO_2 solubility, high thermal stability and low regeneration energy [5,6]. Monoethanolamine (MEA) is the most popular solvent for the uptake of CO_2 due to fast reaction kinetics with CO_2, high alkalinity and low cost. However, there are several drawbacks such as corrosion of equipment, high regeneration energy, oxidative degradation and high volatility [7]. Therefore, a need exists to find and develop new solvents with high absorption performance for CO_2 capture. One of several efficient solvent candidates for CO_2 capture processes is aqueous carbonate solutions, particularly potassium carbonate (K_2CO_3). Aqueous K_2CO_3 solution for the post combustion CO_2 capture has gained widespread attention [8]. In comparison with alkanolamines, potassium carbonate has a number of advantages such as less solvent losses, lower toxicity and better resistance to degradation in the presence of oxygen [9]. In addition, potassium carbonate is able to absorb other components such as SO_x and NO_x existing in flue gas [10]. The most important advantage of potassium carbonate is lower regeneration energy in comparison with MEA, which means a more efficient and economical regeneration process [11]. However, the drawback associated with potassium carbonate is its slow CO_2 absorption rate [12]. In the industrial application, to solve this problem, potassium carbonate solution is usually mixed with an additive to enhance the CO_2 absorption rate [11]. Thus, many researchers investigated the effect of the addition of additives to potassium carbonate in their studies. Bhosale et al. [13] studied kinetic of CO_2 absorption in K_2CO_3 blended with different concentrations of ethylaminoethanol (EAE). Their results indicated the rate increases with the increasing temperature and concentration of EAE in blended solution. Fu and Xie [14] measured viscosity and solubility of CO_2 in tetramethylammonium glycinate ([N1111][Gly]) promoted potassium carbonate solution between 303 and 323 K. Mondal et al. [15] investigated CO_2 solubility and heat of absorption of dipropylenetriamine (DPTA) blend with potassium carbonate in the range of 303-323 K at a total concentration of 30 wt%. They concluded that the mixture of DPTA with potassium carbonate has a lower heat of absorption compared to pure DPTA solution. Lee et al. [16] added potassium glycinate (K-Gly) to potassium carbonate to improve CO_2 absorption. They indicated that the CO_2 partial pressure decreases as the K-Gly concentration increases. Shen et al. [17] used potassium carbonate solution promoted with 5 wt% arginine for CO_2 absorption at different temperatures from 323 to 343 K. They observed that K_2CO_3+arginine has a better CO_2 absorption performance than pure potassium car-

†To whom correspondence should be addressed.
E-mail: rouzbeh.ramezani@edu.unige.it

bonate. Kim et al. [18] reported CO_2 solubility data in a mixture of K_2CO_3 with piperazine (PZ) and 2-methylpiperazine as a promoter at 313, 333 and 353 K, and found that an increase in concentration of the promoter leads to a higher absorption rate. Jo et al. [19] evaluated density and loading capacity of CO_2 in K_2CO_3+sarcosine at pressure and temperature ranging from 0.1 to 1,500 kPa and 353 to 393 K, respectively. According to their findings, absorption capacity of blend solutions decreases with an increase in the mole fraction of amino acid salt. Thee et al. [20] studied CO_2 absorption with monoethanolamine promoted potassium carbonate solution and showed that the addition of MEA accelerates CO_2 absorption rate. Cullinane and Rochelle [21] used K_2CO_3 promoted by PZ for CO_2 absorption. They investigated absorption rate and heat of absorption of K_2CO_3+PZ system from 313-353 K. They observed that rate of absorption and heat of absorption increase with the addition of piperazine.

In this work, three amines, including two amino acids and one diamine were added as potential additives to potassium carbonate solution. The three additives examined in this work were potassium alaninate (K-Ala), potassium serinate (K-Ser) and aminoethylethanolamine (AEEA). The CO_2 absorption capacity of these blend solutions was measured using vapor-liquid equilibrium setup. A correlation for predicting of CO_2 solubility was also presented. The absorption rate of CO_2 into K_2CO_3 promoted by additives was determined at 313 K using a fall in pressure method. In addition, heat of CO_2 absorption of K_2CO_3+additive system was calculated, and results compared to other conventional amines. The main objective of the present study was to develop a novel type of solvents with high absorption performance for post-combustion CO_2 capture.

REACTION SCHEME

1. Reaction of CO_2 with AEEA

The alkanolamines absorb CO_2 via chemical reaction. AEEA react with carbon dioxide in the aqueous phase [22]:

$$2H_2O \leftrightarrow H_3O^+ + OH^- \quad (1)$$

$$CO_2 + 2H_2O \leftrightarrow HCO_3^- + H_3O^+ \quad (2)$$

$$HCO_3^- + H_2O \leftrightarrow CO_3^{2-} + H_3O^+ \quad (3)$$

$$AEEAH^+ + H_2O \leftrightarrow AEEA + H_3O^+ \quad (4)$$

$$^+HAEEAH^+ \leftrightarrow AEEH^+ + H^+ \quad (5)$$

$$AEEA + CO_2 + H_2O \leftrightarrow AEEACOO_p^- + H_3O^+ \quad (6)$$

2. Reaction of CO_2 with Alanine and Serine

Alanine and serine exist in zwitterionic, acidic and deprotonated form. The deprotonated state of these amino acids is more reactive toward carbon dioxide in comparison with two other states [11]. Reaction alanine and serine with CO_2 can be described on the basis of zwitterionic mechanism [19]. In this work, potassium hydroxide (KOH) as a strong base was added to alanine and serine in order to obtain deprotonation of the zwitterionic amino acids.

$$^-OOC-R-NH_3^+ + KOH \rightarrow K^+ + {}^-OOC-R-NH_2 + H_2O \quad (7)$$

$$HO_2CRNH_3^+ \leftrightarrow {}^-O_2CRNH_3^+ \leftrightarrow {}^-O_2CRNH_2 \quad (8)$$

$$NH_2RCOOH + H_3O^+ \leftrightarrow NH_3^+RCOOH + H_2O \quad (9)$$

$$NH_3^+RCOOH + H_2O \leftrightarrow NH_3^+RCOO^- + H_3O^- \quad (10)$$

$$NH_3^+RCOO^- + H_2O \leftrightarrow NH_2RCOO^- + H_3O^+ \quad (11)$$

$$CO_2 + 2NH_2RCOO^- \leftrightarrow COO^-NHRCOO^- + NH_3^+COO^- \quad (12)$$

3. Reaction of CO_2 with K_2CO_3

The reactions involved in the system of K_2CO_3+H_2O+CO_2 can be represented as follows [23]:

Hydrolysis of K_2CO_3:

$$K_2CO_3 + H_2O \leftrightarrow 2K^+ + HCO_3^- + OH^- \quad (13)$$

Ionization of water:

$$2H_2O \leftrightarrow H_3O^+ + OH^- \quad (14)$$

Bicarbonate formation:

$$OH^- + CO_2 \leftrightarrow HCO_3^- \quad (15)$$

Carbonate formation:

$$HCO_3^- + OH^- \leftrightarrow CO_3^{2-} + H_2O \quad (16)$$

The overall reaction for the CO_2 absorption into a solution of potassium carbonate is described as follows [24]:

$$CO_2 + K_2CO_3 + H_2O \leftrightarrow 2KHCO_3 \quad (17)$$

MATERIALS AND METHODS

1. Materials

The AEEA (>99.0% pure), alanine (>99.0% pure), serine (>99% pure), KOH (>85% pure), K_2CO_3 (>99% pure) and MEA (>99.0% pure) were purchased from Acros Organics. In blend solution systems, K_2CO_3 concentration was taken as 2 kmol/m^3 (fixed in all experiments) and concentration of additive was 0.1, 0.2 and 0.3 kmol/m^3.

2. CO_2 Loading Capacity Measurement

Screening tests were performed in a stirred cell reactor to investigate the absorption performance of CO_2 as shown in Fig. 1. This setup consists of several main parts such as N_2 and CO_2 gas cylinder, water bath, glass reactor, pressure and temperature sensor. The procedure and measurement method used in this work were similar to our previous works [25-29]. The pressure and temperature of reactor and gas storage tank were controlled and recorded using a pressure transducer and temperature indicator. First, the reactor was flashed with N_2 gas to remove the residual gases in the reactor. After that, solvent was entered into the reactor and the solution was allowed to attain the desired temperature. Then, CO_2 gas was fed into a gas storage tank from gas cylinder and its total moles could be determined:

$$n_{CO_2} = \frac{[P_1 - P_2]V_s}{RT} \quad (18)$$

The reactor content was then agitated and the pressure in the reactor was decreased over time due to absorption of CO_2 in solvent. The equilibrium state is considered when the pressure values in the reactor was constant. The moles of CO_2 remaining in reactor are calculated by:

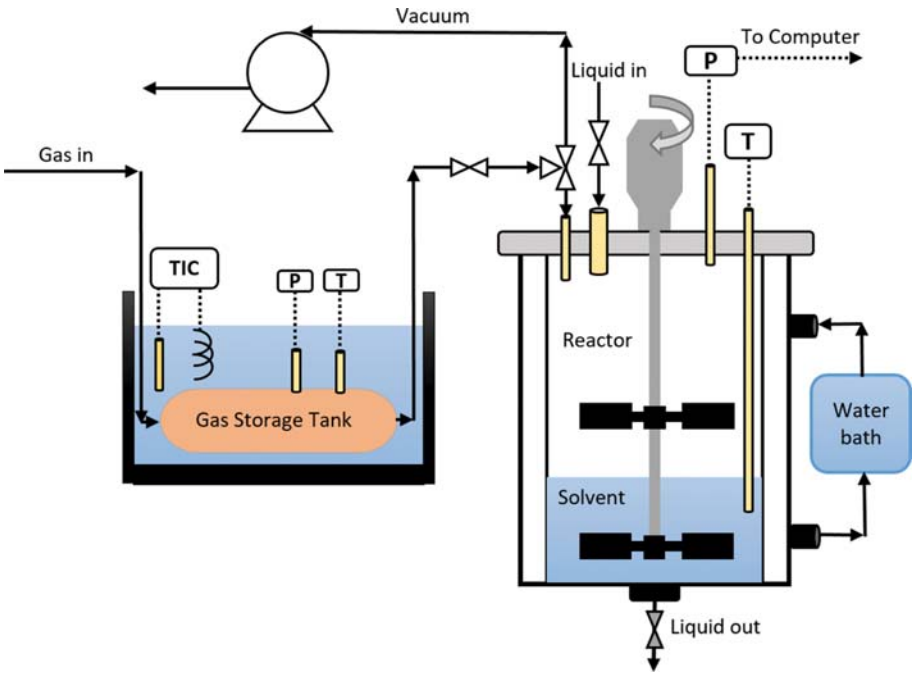

Fig. 1. Schematic diagram of a vapor-liquid equilibrium equipment.

$$P^{e}_{CO_2} = P_F - P_V \quad (19)$$

$$n^{r}_{CO_2} = \frac{VP^{e}_{CO_2}}{RT} \quad (20)$$

where P_V and P_F are the vapor pressure of solution and final pressure of CO_2 in the reactor, respectively. Fall in the pressure of the reactor was continuously recorded and the "P_{CO_2} vs t" data was plotted. Finally, the CO_2 loading capacity (α) can be calculated by Eq. (21):

$$\alpha_{CO_2} = \frac{n_{CO_2} - n^{r}_{CO_2}}{n_{solvent}} \quad (21)$$

Three repeat runs were carried out for each experiment to check the reproducibility of the experimental data. This method has been widely used in other publications [30-33].

3. Absorption Rate Measurement

To measure CO_2 absorption rate using a stirred cell reactor, only the pressure decrease versus time is necessary [34]. This method was widely used previously by many researchers [35-38]. Therefore, this setup was applied to measure the absorption rate of CO_2 in K_2CO_3+additive solutions. The measurement method for absorption rate was given in detail in our previous work [29]. The pressure drop in the reactor was recorded every second and values of absorption rate in K_2CO_3+additive were calculated from Eq. (22):

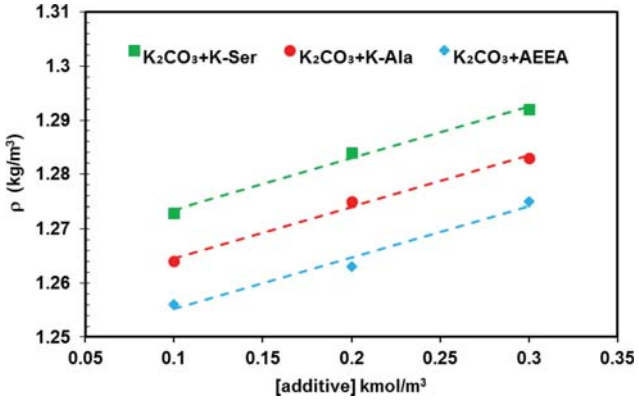

Fig. 2. Density of solutions of K_2CO_3+additive at 313.15 K.

$$N_{CO_2} = \frac{V}{RTA}\frac{dP_{CO_2}}{dt} \quad (22)$$

RESULTS AND DISCUSSION

1. Density

The density data are important for kinetic study and modeling CO_2 absorption process. Thus, density of K_2CO_3+AEEA solutions,

Table 1. The values of densities of solutions of K_2CO_3+additive at 313.13 K

	ρ (kg m^{-3})		
[additive] kmol/m^3	K_2CO_3+AEEA	K_2CO_3+K-Ala	K_2CO_3+K-Ser
0.1	1.256	1.264	1.273
0.2	1.263	1.275	1.284
0.3	1.275	1.283	1.292

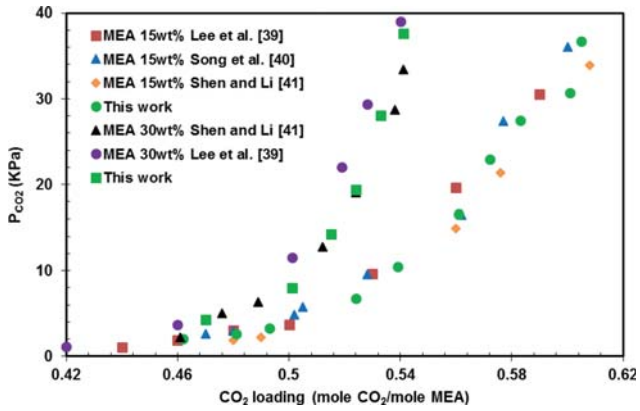

Fig. 3. The CO_2 loading in 15.3 and 30 wt% MEA solution at 313.15 K.

K-Ser and K-Ala was measured using of calibrated pycnometers at three different concentrations as given in Table 1 and presented in Fig. 2. The uncertainty of measurement was 0.001 g/cm^3. As can be observed in Fig. 2, density of solutions increase with the increase of concentration of additive at 313.15 K. In addition, K_2CO_3+K-Ser showed the highest density while K_2CO_3+AEEA has lowest density.

2. CO_2 Solubility in K_2CO_3+Additives

The experimental procedures and reliability of the apparatus have been checked with solutions of 2.5 (15.3 wt%) and 4.98 (30 wt%) kmol/m^3 MEA. According to Fig. 3, the measured CO_2 solubility in this study is in good agreement with those published in the literature at 313 K [39-41].

The CO_2 solubility values in new absorbents are one of the most important parameters for an ideal solvent because they present useful information for the design of CO_2 absorption in post combustion CO_2 capture process [7]. Therefore, the CO_2 absorption capacity in solutions of K_2CO_3 blended with additives was measured at 313 K and CO_2 partial pressures up to 18 kPa. In addition, absorption performance of these blend solutions was compared with results of 2 M K_2CO_3 reported by Tosh et al. [42]. The results of the measurement of the CO_2 solubility in the blend solutions are presented in Figs. 4(a)-(c) and summarized in Tables 2-4.

As illustrated in Figs. 4(a)-(c), all of the blend solutions showed a higher CO_2 loading capacity in comparison with pure K_2CO_3. This is because the amino groups in the AEEA, K-Ala and K-Ser are reactive and can absorb CO_2 [43]. It was also found that the CO_2 absorption capacity is the highest in K_2CO_3+AEEA and the

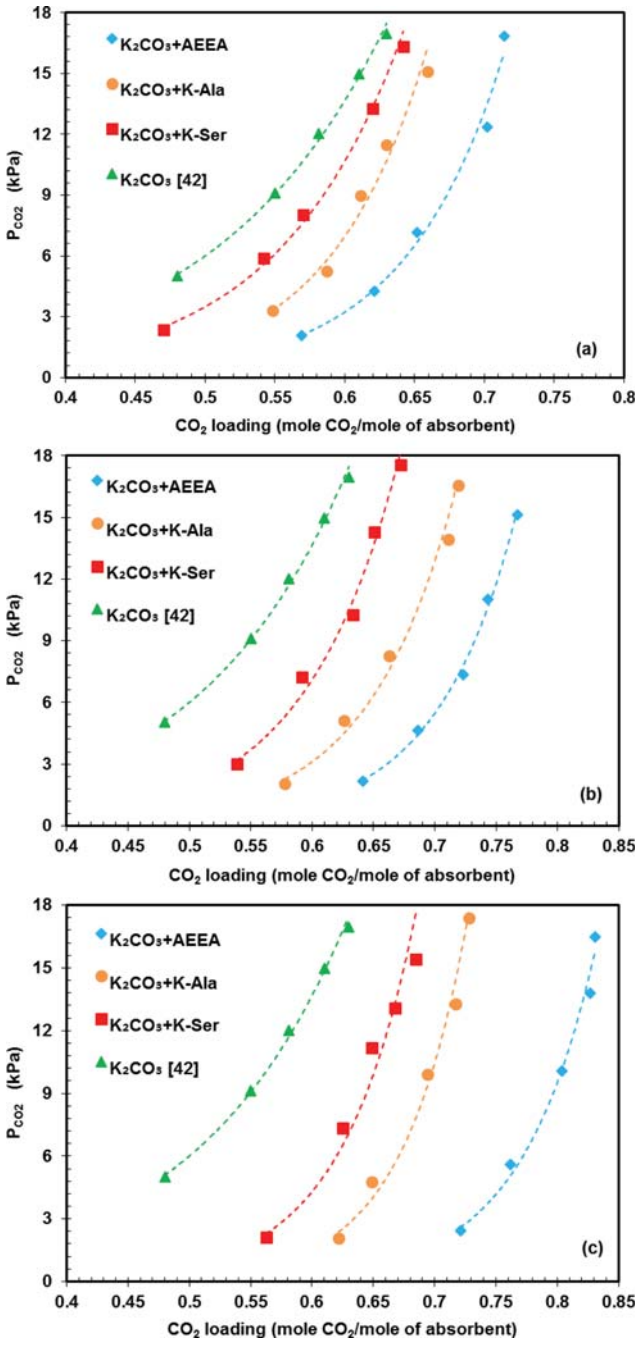

Fig. 4. (a)-(c) The CO_2 loading in K_2CO_3+additive at 313.15 K and at three additive concentrations, (a) 0.1, (b) 0.2, (c) 0.3.

Table 2. CO_2 loading in solution of 2 M K_2CO_3+0.1 M additive at 313 K

2 M K_2CO_3+0.1 M AEEA		2 M K_2CO_3+0.1 M K-Ala		2 M K_2CO_3+0.1 M K-Ser	
P_{CO_2} (kPa)	α	P_{CO_2} (kPa)	α	P_{CO_2} (kPa)	α
02.07	0.569	03.31	0.548	02.37	0.470
04.27	0.621	05.26	0.587	05.88	0.542
07.14	0.652	08.99	0.611	08.02	0.571
12.36	0.702	11.47	0.630	13.28	0.619
16.83	0.714	15.08	0.659	16.31	0.642

Uncertainties: U(T)=±0.01 K; U(P)=±0.1 kPa; U(α)=±0.001

Table 3. CO_2 loading in solution of 2 M K_2CO_3+0.2 M additive at 313 K

2 M K_2CO_3+0.2 M AEEA		2 M K_2CO_3+0.2 M K-Ala		2 M K_2CO_3+0.2 M K-Ser	
P_{CO_2} (kPa)	α	P_{CO_2} (kPa)	α	P_{CO_2} (kPa)	α
02.18	0.641	02.04	0.578	03.01	0.539
04.64	0.686	05.11	0.626	07.22	0.592
07.33	0.723	08.25	0.663	10.25	0.633
11.03	0.743	13.94	0.711	14.30	0.651
15.12	0.767	16.55	0.719	17.55	0.672

Uncertainties: U(T)=±0.01 K; U(P)=±0.1 kPa; U(α)=±0.001

Table 4. CO_2 loading in solution of 2 M K_2CO_3+0.3 M additive at 313 K

2 M K_2CO_3+0.3 M AEEA		2 M K_2CO_3+0.3 M K-Ala		2 M K_2CO_3+0.3 M K-Ser	
P_{CO_2} (kPa)	α	P_{CO_2} (kPa)	α	P_{CO_2} (kPa)	α
02.44	0.721	02.06	0.622	02.10	0.563
05.59	0.762	04.77	0.649	07.33	0.625
10.07	0.804	09.93	0.694	11.18	0.649
13.81	0.827	13.26	0.717	13.06	0.668
16.50	0.831	17.41	0.728	15.42	0.685

Uncertainties: U(T)=±0.01 K; U(P)=±0.1 kPa; U(α)=±0.001

lowest in K_2CO_3+K-Ser solution. This can be because K-Ala and K-Ser have fewer amino groups than AEEA in their molecular structure [44]. The 2 M K_2CO_3+0.3 M AEEA showed the highest CO_2 solubility equal to 0.83 at 313.15 K. However, K_2CO_3+K-SER and K_2CO_3+K-Ala presented lower CO_2 absorption capacity than K_2CO_3+AEEA, but they have higher absorption capacity compared to pure K_2CO_3 solution. In addition, solution of K_2CO_3+K-Ala showed a higher absorption capacity than K_2CO_3+K-Ser solution. This result can be explained mainly due to the fact that alanine as a sterically hindered amino acid has a methyl group at its α-carbon, which leads to an increase at CO_2 loading capacity in comparison with serine [45]. Serine and alanine as amino acids have several advantages, including better resistance to the oxidative degradation, low vapor pressure and high surface tension [46]. As seen in Tables 2-4, the CO_2 solubility in K_2CO_3+additive increases with increasing the concentration of additive. As shown in Figs. 4(a)-(c), with increasing CO_2 partial pressure, the CO_2 loading increases at constant temperature and concentration because of the increase in the driving force [47]. According to experimental results, the loading capacity of CO_2 in these absorbents can be ranked as follows: K_2CO_3+AEEA>K_2CO_3+K-Ala>K_2CO_3+K-Ser>K_2CO_3. Based on these observations, the addition of AEEA, K-Ala and K-Ser as an additive to K_2CO_3 solution will have a significant effect on the CO_2 absorption capacity. In addition, the CO_2 solubility in 2 M K_2CO_3+0.2 M K-Ala at three temperatures 303, 313 and 323 K was measured. Since reaction would shift in the backward direction with increasing temperature, the CO_2 solubility in absorbent decreases [18].

The CO_2 solubility for 2 M K_2CO_3+0.3 M AEEA system is plot-

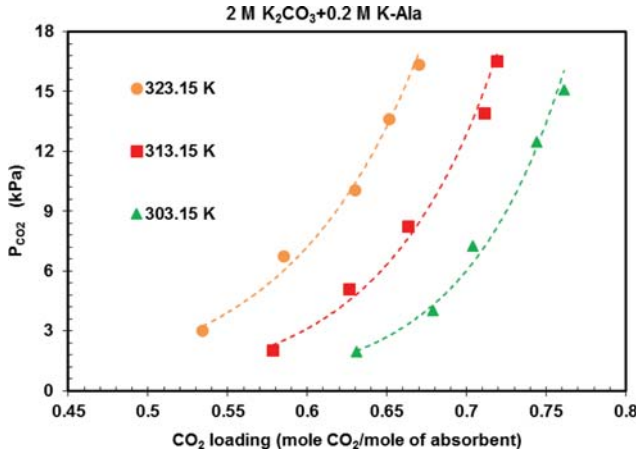

Fig. 5. Effect of temperature on CO_2 loading in 2 M K_2CO_3+0.2 M K-Ala solution.

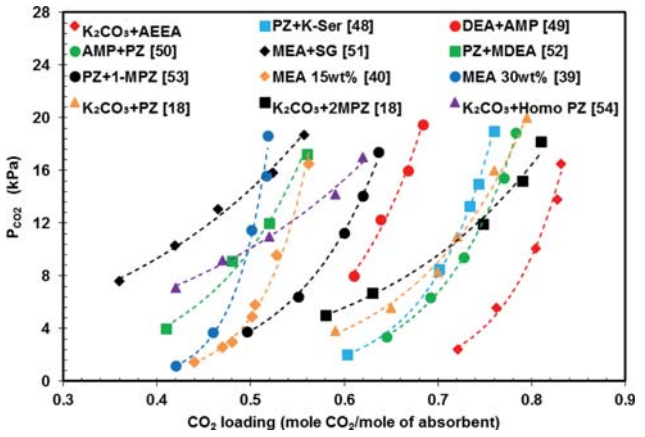

Fig. 6. Comparison of CO_2 loading in 2 M K_2CO_3+0.3 M AEEA with the other blend solutions at 313.15 K.

ted in Fig. 6, and its absorption performance was compared to the CO_2 solubility in MEA solution as a widely used solvent in post combustion CO_2 capture [48-54] at the same experimental condition. The comparison showed that the mixture of K_2CO_3+AEEA suggested in this work has the highest CO_2 solubility and the MEA+SG has shown the least CO_2 solubility at 313.15 K. The high absorption performance of K_2CO_3+AEEA solution can be related to their structural feature. AEEA is a diamine with one secondary and one primary amine group in its structure [22]. Thus, one mole of AEEA can absorb two moles of CO_2 which is higher than absorbents such as PZ, AMP, MEA, DEA and MDEA. Ma'mun et al. [22] studied CO_2 absorption capacity and absorption rate of AEEA solution and discovered that AEEA has better absorption performance compared to MEA, DEA, PZ and glycine. Therefore, its blend with K_2CO_3 solution, an absorbent with high absorption capacity, exhibits higher CO_2 solubility compared to other absorbents presented in Fig. 6. MEA+SG solution shows the lowest CO_2 loading; however, its performance is better than pure MEA at high CO_2 partial pressures. After K_2CO_3+AEEA, the K_2CO_3+2MPZ and AMP+PZ solutions have highest CO_2 absorption capacity. Kim et al. [18] studied CO_2 solubility in solutions of K_2CO_3+2MPZ and K_2CO_3+PZ, and concluded that CO_2 solubility in K_2CO_3+2MPZ solution is higher than K_2CO_3+PZ solution at partial pressures higher than 10 kPa. The high CO_2 absorption capacity in these solutions is caused by two amino groups in structures of 2MPZ and PZ which react with CO_2 and lead to a significant increase in CO_2 absorption capacity. In addition, we found that AMP+PZ solution is a better choice than K_2CO_3+2MPZ solution at low partial pressure of CO_2. The sterically hindered amines, e.g., AMP, have advantages such as good selectivity, high degradation resistance, low volatility and low corrosion rate [50]. It is also observed that the PZ+K-Ser solution presents better absorption performance than MEA and DEA+AMP. The low CO_2 absorption capacity of MEA and DEA is one of the limitations of these solutions. MEA and DEA as primary and secondary alkanolamines have fewer amino groups than PZ and that explains their poor performance [40].

3. Correlation of Experimental Data

The predictive correlations for CO_2 solubility are useful since they can be used to determine the CO_2 loading without experimental test at different operating conditions. In this work, the CO_2 loading capacity data were correlated using response surface methodology. The following equation satisfactorily fits the experimental CO_2 solubility data for K_2CO_3+additive solution:

$$CO_2\ \text{Solubility}=a_0+a_1\,T+a_2\,P+a_3\,C+a_4\,T\times P+a_5\,T\times C+a_6\,P\times C+a_7\,T^2+a_8\,P^2+a_9\,C^2 \quad (23)$$

where T is temperature (K), P is CO_2 partial pressure (kPa), C is additive concentration in blended solutions and a_0 to a_9 are the constant coefficients which were listed in Table 5. The predicted values by the correlation were compared to experimental CO_2 solubility data. According to Fig. 7, good agreement was observed. The average deviation between the experimental solubility data and the predicted values was obtained using Eq. (24) and were presented equal to 1.02%, 0.88% and 0.78% for K_2CO_3+AEEA, K_2CO_3+K-Ala and K_2CO_3+K-Ser, respectively.

$$\%AAD=100\times\frac{1}{n}\Sigma_{i=1}^{i=n}\left|\frac{\alpha_{exp}-\alpha_{cor}}{\alpha_{exp}}\right| \quad (24)$$

Table 5. The values of constant coefficients in Eq. (23)

Coefficient	K_2CO_3+AEEA	K_2CO_3+K-Ala	K_2CO_3+K-Ser
a_0	−0.75979	−1.82025	4.39217
a_1	0.010343	0.01980	−0.02129
a_2	9.90748×10^{-3}	-3.19032×10^{-3}	1.76617×10^{-3}
a_3	1.85300	−0.61947	0.61086
a_4	2.80915×10^{-18}	3.61842×10^{-5}	1.64474×10^{-5}
a_5	-3.75000×10^{-3}	2.12500×10^{-3}	-1.62500×10^{-3}
a_6	-3.42105×10^{-3}	-4.93421×10^{-3}	-1.51316×10^{-3}
a_7	-2.04193×10^{-5}	-3.94763×10^{-5}	2.83202×10^{-5}
a_8	-9.20190×10^{-5}	-6.05138×10^{-5}	-5.93260×10^{-5}
a_9	−0.34853	0.61560	0.34094

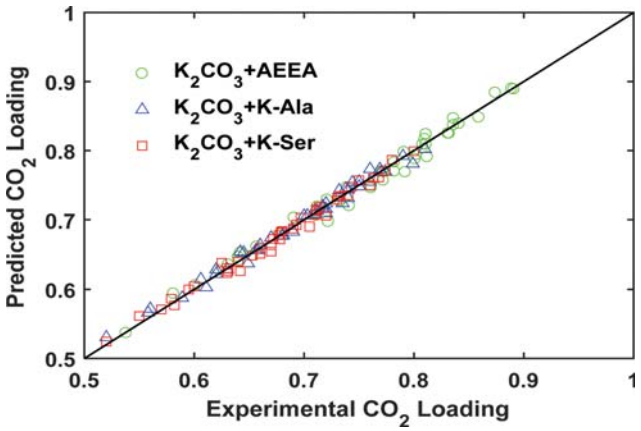

Fig. 7. Predicted CO_2 solubility data points versus experimental data for K_2CO_3+additive system.

4. CO_2 Absorption Rate in K_2CO_3+Additives

As already mentioned, the main drawback with K_2CO_3 solution is the low absorption rate compared to amines. Thus, improving the absorption rate of K_2CO_3 as a suitable solvent is important for reducing size and cost. The effect of the addition of AEEA, K-Ala and K-Ser to K_2CO_3 was investigated and compared to pure K_2CO_3 solution at 313.15 K. The slope of the CO_2 absorption capacity curves versus time was used to evaluate CO_2 absorption rate in K_2CO_3+additive system. According to Fig. 8(a)-(c), promoted K_2CO_3 solutions showed higher absorption rate than pristine K_2CO_3 solution. Actually, CO_2 absorption rate can be accelerated remarkably when K_2CO_3 solution is promoted by the addition of small amounts of the suggested additives. The pH of absorbent increases, when AEEA, K-Ala or K-Ser are added to K_2CO_3. Therefore, rate of reaction CO_2 with OH^- increases, which causes an enhancement in the overall absorption rate [11]. The rate of absorption for the K_2CO_3+AEEA was also observed to be faster compared to K_2CO_3+K-Ala and K_2CO_3+K-Ser because of fast kinetic of primary amino group in AEEA structure with CO_2. In addition, rate in K_2CO_3+K-Ser solution is higher than K_2CO_3+K-Ala solution. Compared to K-Ala, K-Ser has a primary amino group and also a hydroxymethyl group which is attached to α-carbon, hence a fast reaction with CO_2 is

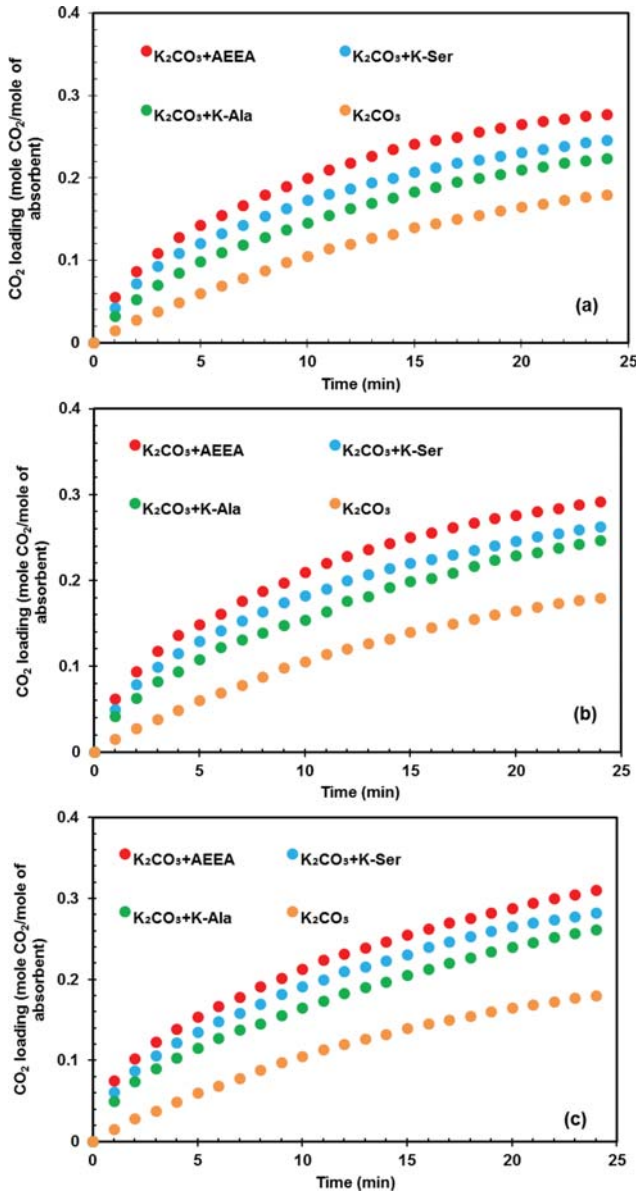

Fig. 8. (a)-(c) CO_2 loading as a function of absorption time for K_2CO_3+additive at 313.15 K and at three additive concentrations, (a) 0.1, (b) 0.2, (c) 0.3 kmol/m^3.

expected [55]. Therefore, CO_2 absorption rate ranks as follows: K_2CO_3+AEEA>K_2CO_3+K-Ser>K_2CO_3+K-Ala>K_2CO_3.

It is clearly seen from Fig. 9, that at constant concentration, absorption rate of CO_2 was accelerated when temperature increased because of increase at reaction rate constant. A similar trend was

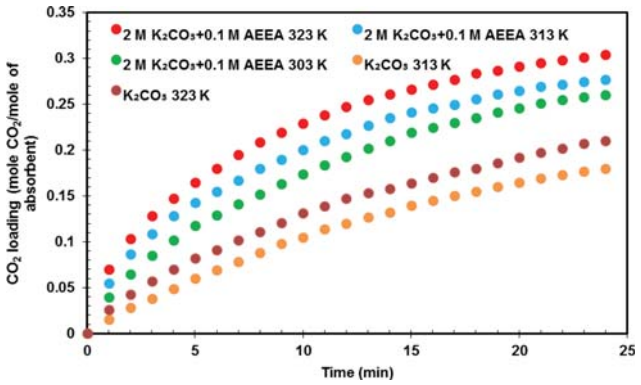

Fig. 9. Effect of the temperature on the CO_2 absorption rate in 2 M K_2CO_3+0.1 M AEEA solution.

observed for the K_2CO_3+K-Ala and K_2CO_3+K-Ser.

For further investigation, CO_2 absorption rate of K_2CO_3+additive solution was calculated using Eq. (22) at 313.15 K, and results presented in Table 6-8. Pressure decay during absorption of CO_2 in K_2CO_3+additive systems at different temperatures and concentrations was obtained using a pressure sensor. Thus, the CO_2 absorption rate of K_2CO_3+additive was obtained from the slope of the plot of pressure versus time, and Eq. (22). It was found from Table 6-8 that the CO_2 absorption rate has higher values at higher additive concentration because the reaction rate between CO_2 and additives increase, which leads to an enhancement at overall absorption rate.

Fig. 10 shows a comparison between the absorption rate in 2 M K_2CO_3+0.3 M AEEA which has highest absorption rate compared to other blend solutions studied in the literature [56-62] at 313.15 K. It was found that CO_2 absorption rate of K_2CO_3+AEEA solution was higher than other absorbents except for K_2CO_3+EAE solution. According to Ma'mun et al. [22], reaction order with respect to AEEA is equal to two, which is higher than reaction order with respect to MEA, PZ, PZEA, DEA, MDEA, arginine, glycine and AMP, and consequently, an increase in concentration of AEEA has further effect on enhancement of absorption rate compared to the other absorbents. In addition, as mentioned in section 4.2, primary and secondary amine groups in AEEA structure react with CO_2 and form primary and secondary carbamates with high pKa. This can lead to a significant enhancement in CO_2 absorption rate of AEEA+K_2CO_3 system [22]. Bhosale et al. [13] added EAE to K_2CO_3 solution at 303.15 K and observed that the CO_2 absorption rate increases from 0.5×10^6 to 6×10^6 kmol/m^{2}s. EAE has a high pKa value which directly affects the absorption rate. Therefore, it was expected that its absorption rate was better than other

Table 6. Absorption rate of CO_2 in solution of 2 M K_2CO_3+0.1 M additive

	2 M K_2CO_3+0.1 M AEEA	2 M K_2CO_3+0.1 M K-Ser	2 M K_2CO_3+0.1 M K-Ala
T (K)	$N_{CO_2}\times10^6$ (kmol/m^2·s)		
303.15	3.04	2.38	1.94
313.15	4.71	3.91	3.05
323.15	6.26	5.13	4.22

Table 7. Absorption rate of CO_2 in solution of 2 M K_2CO_3+0.2 M additive

	2 M K_2CO_3+0.2 M AEEA	2 M K_2CO_3+0.2 M K-Ser	2 M K_2CO_3+0.2 M K-Ala
T (K)		$N_{CO_2}\times10^6$ (kmol/m^2·s)	
303.15	3.85	2.98	2.47
313.15	5.79	4.55	3.81
323.15	7.15	5.96	5.02

Table 8. Absorption rate of CO_2 in solution of 2 M K_2CO_3+0.3 M additive

	2 M K_2CO_3+0.3 M AEEA	2 M K_2CO_3+0.3 M K-Ser	2 M K_2CO_3+0.3 M K-Ala
T (K)		$N_{CO_2}\times10^6$ (kmol/m^2·s)	
303.15	4.43	3.78	3.26
313.15	7.02	5.38	4.43
323.15	7.95	6.77	5.89

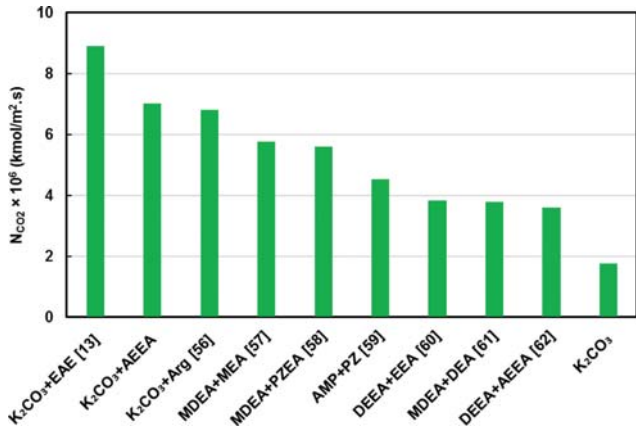

Fig. 10. Comparison of CO_2 absorption rate between 2 M K_2CO_3+ 0.3 M AEEA solution with other absorbent studied in literature at T=313 K and P_{CO_2}=15 kPa.

absorbents. Arginine as an amino acid with a primary amino group was selected by Shen et al. [56] to improve reaction kinetics of CO_2 in K_2CO_3. Arginine actually acted as an effective promoter and increased absorption rate by 40%. PZ and PZEA are known to have fast reaction kinetics because of rapid carbamate formation [58]. For this reason, Sun et al. [59] added PZ as a rate promoter to AMP solution. AMP has lower absorption rate than MEA because it forms the bicarbonate, which reduces the reaction rate. However DEA showed the absorption rate better than K_2CO_3, but its rate is lower than MEA. The two hydroxyl groups in structure of DEA reduce the carbamate stability and pKa, which leads to a decrease in absorption rate [61]. Pawlak [62] improved absorption rate of CO_2 in DEEA as a tertiary amine by addition of AEEA and observed that AEEA significantly increases absorption rate. The results presented in this work show that the addition of amine additives to potassium carbonate improves the CO_2 absorption rate significantly and acts as a potential activator for pure potassium carbonate.

5. Heat of Absorption

An important process parameter in a gas treating process using chemical absorbents is calculation of absorption heat since it is directly related with energy consumption in the stripper for regeneration of absorbent [63]. The values of heat of absorption can be obtained experimentally using a calorimeter or calculated on the basis of the following the Gibbs-Helmholtz equation [64]:

$$-\frac{\Delta H}{R}=\left(\frac{\partial \ln P_{CO_2}}{\partial(1/T)}\right)_{\alpha} \tag{25}$$

where R, T, α and ΔH are gas constant, temperature of system, CO_2 loading capacity and heat of absorption (kJ/mol CO_2), respectively. α is defined as the mole of absorbed CO_2 per mole of absorbent. Carson et al. [65] measured heat of CO_2 absorption of DEA, MDEA and MEA solutions using a calorimeter. Lee et al. [66], Rho et al. [67] and Li et al. [68] calculated heat of CO_2 absorption of these solutions using the Gibbs-Helmholtz equation. They compared their results with values measured by Carson and found that Eq. (25) gives a good agreement with experimental results. Thus, applying Gibbs-Helmholtz equation to calculate heat of absorption is reliable [69]. Many researchers have used this measurement method in their works [70-75]. We used the Gibbs-Helmholtz equation to estimate heat of CO_2 absorption of 2 M K_2CO_3 promoted by (0.1-0.3 M) AEEA, K-Ala and K-Ser. The absorption heat was calculated directly from the slope of plot of $\ln P_{CO_2}$ versus 1/T at constant CO_2 solubility. Before measurement of heat absorption suggested in this study, ΔH of MEA, MDEA and AEEA were measured and results compared with the literature to ensure the reliability of the experimental results. It was found that the values measured in this study were close to data reported in the literature with 2.1% uncertainty. After validation of method, heat of CO_2 absorption of K_2CO_3+additive was calculated and results given in Tables 9-11. The results in these tables show that an increase in CO_2 loading capacity leads to a decrease in heat of absorption in K_2CO_3+additive system. This is because at higher loading capacity, the physical absorption dominates, and bicarbonate forms, which leads to a reduction at heat of CO_2 absorption [76]. A similar trend was observed by Cullinane et al. [21] for K_2CO_3+PZ and Kim et al. [12] for K_2CO_3+2MPZ solution.

Absorption heat of K_2CO_3+additive solutions tested in this work was compared to more commonly used solvents in the CO_2 absorption processes, such as MEA [45], AMP [77], PZ [78], DEA [77], MDEA [79] and blend of K_2CO_3 with other additives such as

Table 9. Heat of CO_2 absorption in solution of 2 M K_2CO_3+0.1 M additive

	2 M K_2CO_3+0.1 M AEEA	2 M K_2CO_3+0.1 M K-Ala	2 M K_2CO_3+0.1 M K-Ser
α	$-\Delta H$ (kJ/mol CO_2)	$-\Delta H$ (kJ/mol CO_2)	$-\Delta H$ (kJ/mol CO_2)
0.50	44.01	37.22	39.98
0.55	43.89	36.47	39.04
0.60	43.12	35.89	38.15
0.65	42.23	35.04	37.42
0.70	41.04	34.26	36.57
0.75	40.33	33.51	35.83
0.80	39.50	32.79	35.02

α (mole CO_2/mole of absorbent) is the moles of CO_2 absorbed per one mole of solvent

Table 10. Heat of CO_2 absorption in solution of 2 M K_2CO_3+0.2 M additive

	2 M K_2CO_3+0.2 M AEEA	2 M K_2CO_3+0.2 M K-Ala	2 M K_2CO_3+0.2 M K-Ser
α	$-\Delta H$ (kJ/mol CO_2)	$-\Delta H$ (kJ/mol CO_2)	$-\Delta H$ (kJ/mol CO_2)
0.50	45.79	39.02	41.65
0.55	45.24	38.44	40.86
0.60	44.65	37.53	40.04
0.65	43.72	36.88	39.13
0.70	42.54	36.03	38.27
0.75	41.31	35.46	37.53
0.80	40.97	34.97	36.79

α (mole CO_2/mole of absorbent) is the moles of CO_2 absorbed per one mole of solvent

Table 11. Heat of CO_2 absorption in solution of 2 M K_2CO_3+0.3 M additive

	2 M K_2CO_3+0.3 M AEEA	2 M K_2CO_3+0.3 M K-Ala	2 M K_2CO_3+0.3 M K-Ser
α	$-\Delta H$ (kJ/mol CO_2)	$-\Delta H$ (kJ/mol CO_2)	$-\Delta H$ (kJ/mol CO_2)
0.50	47.34	40.66	43.01
0.55	46.96	39.58	42.36
0.60	46.08	39.02	41.68
0.65	45.12	38.41	41.02
0.70	44.38	37.75	40.14
0.75	43.26	37.04	39.25
0.80	42.06	36.39	38.40

α (mole CO_2/mole of absorbent) is the moles of CO_2 absorbed per one mole of solvent

K_2CO_3+2MPZ [12], K_2CO_3+PZ [21] and K_2CO_3+DPTA [15] as shown in Fig. 11. It was found that a blend of K_2CO_3 with amine additives has lower heat of CO_2 absorption in comparison with pure MEA and other absorbents, which means less energy is needed for CO_2 regeneration in stripper column. However, amines like MEA have fast reaction kinetics, but they have high absorption heat, which increases CO_2 capture cost. K_2CO_3 solution is an attractive absorbent because of its low regeneration energy requirement. Therefore, as expected, a blend of K_2CO_3 as a base solvent with amine additives showed much better performance in terms of heat of absorption compared to conventional amines such as MEA, AMP, PZ, DEA and MDEA. It also can be seen from Fig. 11 that K_2CO_3 blended with AEEA gives a higher value of heat of absorption over the entire CO_2 solubility in comparison with K_2CO_3+K-Ala and K_2CO_3+K-Ser due to the hydroxyl group in the structure of AEEA. Furthermore, the K_2CO_3+K-Ala showed the best performance in terms of heat of absorption. So, a mixture of K_2CO_3 with K-Ala has lowest heat of absorption and can be a favorable candidate for CO_2 capture. A structure similar to sterically hindered amines in alanine, which causes a steric hindrance effect, and also the formation of an unstable carbamate can be reasons for reduction of the heat of absorption in comparison to serine [47]. The ease of regeneration and high absorption capacity are the most important features of sterically hindered amines [77]. Thus, the heat of CO_2 absorption can be ranked as follows: K_2CO_3+K-Ala<K_2CO_3+K-Ser<K_2CO_3+AEEA<MEA. As can be seen in Fig. 11, MEA solution as a primary alkanolamine has highest value of heat of absorption equal to 84.17 kJ/mol CO_2. This may be because MEA reacts

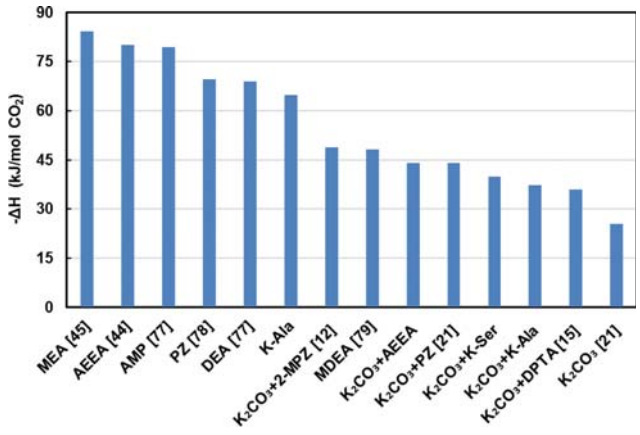

Fig. 11. Comparison of heat of CO_2 absorption of K_2CO_3+additive with the other absorbents.

with CO_2 and forms stable carbamates, which causes an increase in heat of absorption [45]. Chowdhury et al. [77] observed that sterically hindered amines like AMP indicate a better absorption heat performance than MEA because of formation of unstable carbamate. In addition, Fig. 11 shows that PZ solution as a secondary diamines has heat of absorption value lower than AMP and MEA, but higher than DEA and MDEA. It was also found that absorption heat of DEA solution is about 22% lower than MEA [77]. Generally, secondary alkanolamines (DEA) have heats of absorption lower than primary alkanolamines (MEA) and higher than tertiary alkanolamines (MDEA) [77]. However, heat of absorption of MDEA is higher than K_2CO_3, but its value is still lower than other conventional amines such as AMP, DEA, PZ, PZEA and MEA because of formation of bicarbonates instead of carbamates in reaction of CO_2 with MDEA [79]. A comparison of heat of absorption between K_2CO_3 solution and K_2CO_3+PZ and K_2CO_3+2MPZ showed that the addition of these additives increases absorption heat because PZ and 2MPZ have primary and secondary amino groups, which form carbamate. As mentioned, these carbamate ions increase absorption heat; however, absorption heat of these blended solutions is still lower than MEA [21]. Therefore, using K_2CO_3 blended with a potential additive such as AEEA, K-Ala and K-Ser for CO_2 absorption from flue gas is a right choice from the heat of absorption point of view.

A comparison of CO_2 absorption performance of the suggested additives, including AEEA, K-Ala and K-Ser, was carried out to identify the most efficient additive as shown in Fig. 12. This figure shows that the blend of K_2CO_3 and AEEA has the highest CO_2 solubility and rate among the other additives in this work. However, it showed a higher heat of absorption in comparison with K_2CO_3+K-Ala and K_2CO_3+K-Ser, but its value is lower than pure MEA. Aqueous MEA solution has a high reactivity with CO_2, but has the limitation of high regeneration energy and low CO_2 solubility [80]. Alternatively, K_2CO_3 has the high CO_2 absorption capacity and low heat of absorption but low absorption rate. However, we observed that with the addition of AEEA, K-Ala and K-Ser can improve CO_2 absorption rate of K_2CO_3. Therefore, this implies that the blend of K_2CO_3 with additives suggested in this work, there is the opportunity to combine the high absorption rate provided by additives with the high CO_2 absorption capacity and low heat of absorption.

6. Toxicity

An ideal absorbent should have several desired characteristics, including fast kinetics, high absorption capacity and low regeneration energy [5]. In addition, the low environmental and health risks are another characteristics of an ideal solvent for CO_2 capture process [81]. Therefore, the toxicity of solvent should be investigated. The alkanolamines (MEA, DEA, TEA), sterically hindered amines (AMP) and cyclic amines (PZ, PZEA, 2-MPZ) are the most popular absorbents for CO_2 capture process which have high toxicity [82,83]. In comparison with amine-based absorbents, K_2CO_3 solution has lower toxicity [17,84] as shown in Fig. 13. This figure shows values of lethal dose (LD_{50}) of several absorbents [85-100]. The LD_{50} is the amount of a material which causes the death of 50% of a group of tested animals in the certain time [81]. The lower values of LD_{50} means more toxicity. Amino acids used in this study were alanine (Ala) and serine (Ser). In general, amino acid salts have lower toxicity over amines [101,102]. According to Fig. 13, amino acids including His, Ser, Gly, Glu, Ala, Pro and Tau showed the least and conventional amines such as MEA and PZ had the highest toxicity among the various absorbents for CO_2 capture. It also can be seen from Fig. 13 that AEEA presents higher toxicity than amino acids, but its value is still low compared to conventional amines. As an overall conclusion, the absorbents used in

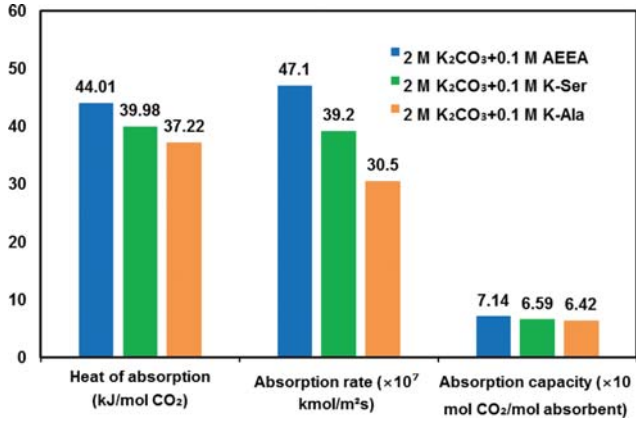

Fig. 12. Comparison of performance of additives studied in this work.

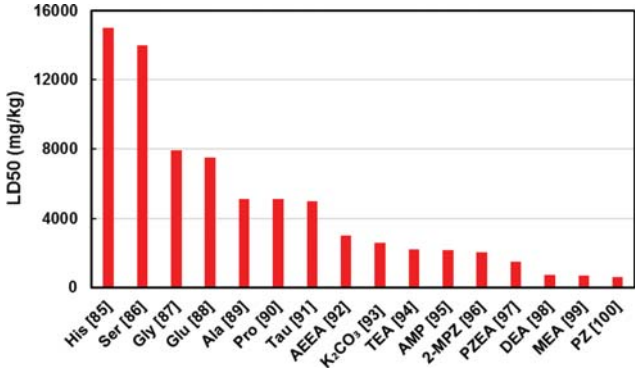

Fig. 13. Comparison of toxicity (LD_{50}) of amines and amino acids.

this study seem to have a better performance in terms of toxicity in comparison with other amines, and therefore could be considered as an environmentally relatively acceptable absorbent.

CONCLUSION

After a prescreening, three promoters including K-Ala, K-Ser and AEEA were selected to add to potassium carbonate to improve its absorption performance. The values of absorption heat, CO_2 loading capacity and absorption rate of CO_2 in these solutions were reported. The experimental results revealed that addition of the suggested additives resulted in a significant increase in CO_2 absorption rate and loading capacity of K_2CO_3 solution. Of all the blend solutions studied, the highest CO_2 absorption rate and solubility were achieved by K_2CO_3+AEEA. Compared to pure MEA, K_2CO_3+ additive systems have lower heat of absorption, which is favorable for the CO_2 capture process. Overall, K_2CO_3 blended with AEEA could be a promising solvent for CO_2 capture process. It is suggested to further investigate corrosion rate, desorption rate and viscosity issues for a complete evaluation of these blend absorbents in this study in order to use in acid gas removal applications.

NOMENCLATURE

K_2CO_3 : potassium carbonate
K-Ala : potassium alaninate
K-Ser : potassium serinate
AEEA : 2-((2-aminoethyl)amino)ethanol
MEA : monoethanolamine
MDEA : methyldiethanolamine
EAE : ethylaminoethanol
K-Gly : potassium glycinate
KOH : potassium hydroxide
TEA : triethanolamine
PZ : piperazine
2MPZ : 2-methylpiperazine
PZEA : 2-(1-piperazinyl)-ethylamine
DEA : diethanolamine
AMP : 2-amino-2-methyl-1-propanol
SG : sodium glycinate
His : histidine
Glu : glutamate
Pro : proline
Tau : taurine
DPTA : dipropylenetriamine
1-MPZ : 1-methyl piperazine
α : CO_2 solubility [mole CO_2/mole of absorbent]
$n_{solvent}$: the moles of solvent in liquid phase

REFERENCES

1. Zh. Liang, K. Fu, R. Idem and P. Tontiwachwuthikul, *Chinese J. Chem. Eng.*, **24**, 278 (2016).
2. R. Ramezani, S. Mazinani, R. Di Felice, S. Darvishmanesh and B. Van der Bruggen, *Int. J. Greenh. Gas Con.*, **62**, 61 (2017).
3. R. Ramazani, S. Mazinani, A. Hafizi, A. Jahanmiri, B. Van Der Bruggen and S. Darvishmanesh, *Sep. Sci. Technol.*, **51**, 327 (2016).
4. A. Setameteekul, A. Aroonwilas and A. Veawab, *Sep. Purif. Technol.*, **64**, 16 (2008).
5. I. Sreedhar, T. Nahar, A. Venugopal and B. Srinivas, *Renew. Sust. Energy Rev.*, **76**, 1080 (2017).
6. R. Ramazani, S. Mazinani, A. Jahanmiri and B. Van Der Bruggen, *Int. J. Greenh. Gas Con.*, **45**, 27 (2016).
7. Sh. Shen, Y. Yang, Y. Wang, Sh. Ren, J. Han and A. Chen, *Fluid Phase Equilib.*, **399**, 40 (2015).
8. G. Hu, K. Smith, Y. Wu, S. Kentish and G. Stevens, *Energy Fuels*, **31**, 4280 (2017).
9. H. Thee, K. Smith, G. da Silva, S. Kentish and G. Stevens, *Chem. Eng. J.*, **181**, 694 (2012).
10. C. Anderson, T. Harkin, M. Ho, K. Mumford, A. Qader, G. Stevens and B. Hooper, *Energy Procedia*, **37**, 225 (2013).
11. H. Thee, N. Nicholas, K. Smith, G. Silva, S. Kentish and G. Stevens, *Int. J. Greenh. Gas Con.*, **20**, 212 (2014).
12. Y. Kim, J. Choi, S. Yun, S. Nam and Y. Yoon, *Korean J. Chem. Eng.*, **33**, 3465 (2016).
13. R. Bhosale, A. Kumar, F. AlMomani, U. Ghosh, A. AlNouss, J. Scheffe and R. Gupta, *Ind. Eng. Chem. Res.*, **55**, 5238 (2016).
14. D. Fu and J. Xie, *J. Chem. Thermodyn.*, **102**, 310 (2016).
15. B. Mondal, S. Bandyopadhyay and A. Samanta, *Chem. Eng. Sci.*, **170**, 58 (2017).
16. A. Lee, M. Wolf, N. Kromer, K. Mumford, N. Nicholas, S. Kentish and G. Stevens, *Int. J. Greenh. Gas Con.*, **36**, 27 (2015).
17. Sh. Shen, X. Feng and Sh. Ren, *Energy Fuels*, **27**, 6010 (2013).
18. Y. Kim, J. Choi, S. Nam and Y. Yoon, *J. Ind. Eng. Chem.*, **18**, 105 (2012).
19. H. Jo, M. Lee, B. Kim, H. Song, H. Gil and J. Park, *J. Chem. Eng. Data*, **57**, 3624 (2012).
20. H. Thee, Y. Suryaputradinata, K. Mumford, K. Smith, G. Silva, S. Kentish and G. Stevens, *Chem. Eng. J.*, **210**, 271 (2012).
21. J. Cullinane and G. Rochelle, *Chem. Eng. Sci.*, **59**, 3619 (2004).
22. S. Ma'mun, V. Dindore and H. Svendsen, *Ind. Eng. Chem. Res.*, **46**, 385 (2007).
23. K. Mumford, K. Smith, C. Anderson, S. Shen, W. Tao and Y. Suryaputradinata, *Energy Fuels*, **26**, 138 (2012).
24. A. Comite, C. Costa, R. Di Felice, P. Pagliai and D. Vitiello, *Korean J. Chem. Eng.*, **32**, 239 (2015).
25. R. Ramazani, A. Samsami, A. Jahanmiri, B. Van der Bruggen and S. Mazinani, *Int. J. Greenh. Gas Con.*, **51**, 29 (2016).
26. S. Mazinani, R. Ramazani, A. Samsami, A. Jahanmiri, B. Van der Bruggen and S. Darvishmanesh, *Fluid Phase Equilib.*, **396**, 28 (2015).
27. R. Ramazani, S. Mazinani, A. Jahanmiri, S. Darvishmanesh and B. Van der Bruggen, *J. Taiwan Inst. Chem. E.*, **65**, 341 (2016).
28. R. Ramezani, S. Mazinani, R. Di Felice and B. Van der Bruggen, *J. Nat. Gas Sci. Eng.*, **45**, 599 (2017).
29. R. Ramezani, S. Mazinani and R. Di Felice, *J. Environ. Chem. Eng.*, **6**, 3262 (2018).
30. M. Taib and T. Murugesan, *Chem. Eng. J.*, **182**, 56 (2012).
31. Z. Feng, F. Cheng-Gang, W. You-Ting, W. Yuan-Tao and L. Min, *Chem. Eng. J.*, **160**, 691 (2010).
32. P. Singh, J. Niederer and G. Versteeg, *Int. J. Greenh. Gas Con.*, **1**, 5 (2007).

33. P. Singh, J. Niederer and G. Versteeg, *Chem. Eng. Res. Des*., **87**, 135 (2009).
34. P. N. Sutar, P. D. Vaidya and E. Y. Kenig, *Chem. Eng. Sci*., **100**, 234 (2013).
35. B. Lu, X. Wang, Y. Xia, N. Liu, S. Li and W. Li, *Energy Fuels*, **27**, 6002 (2013).
36. A. F. Portugal, F. D. Magalhaes and A. Mendes, *Chem. Eng. Sci*., **63**, 3493 (2008).
37. N. P. Elk, S. Fradette and G. F. Versteeg, *Chem. Eng. J*., **259**, 682 (2015).
38. P. N. Sutar, A. Jha, P. D. Vaidya and E. Y. Kenig, *Chem. Eng. J*., **207**, 718 (2012).
39. J. Lee and I. Otto, *J. Appl. Chem. Bio. Technol*., **26**, 541 (1976).
40. J. Song, J. Yoon, H. Lee and K. Lee, *J. Chem. Eng. Data*, **45**, 497 (1996).
41. K. Shen and P. Li, *J. Chem. Eng. Data*, **37**, 96 (1992).
42. J. Tosh, J. Field, H. Benson and W. Haynes, *U. S. Bureau of Mines Rept. Invest*., **5484**, 23 (1959).
43. S. Choi, S. Nam, Y. Yoon, K. Park and S. Park, *Ind. Eng. Chem. Res*., **53**, 14451 (2014).
44. I. Kim and H. Svendsen, *Ind. Eng. Chem. Res*., **46**, 5803 (2007).
45. M. Kim, H. Song, M. Lee, H. Jo and J. Park, *Ind. Eng. Chem. Res*., **51**, 2570 (2012).
46. H. Song, M. Lee, H. Kim, A. Gaur and J. Park, *J. Chem. Eng. Data*, **56**, 1371 (2011).
47. Z. Wu, Z. Huang, Y. Zhang, Y. Qin, J. Ma and Y. Luo, *Chem. Eng. J*., **295**, 64 (2016).
48. D. Kang, S. Park, H. Jo, J. Min and J. Park, *J. Chem. Eng. Data*, **58**, 1787 (2013).
49. G. Kumar, T. Mondal and M. Kundu, *J. Chem. Eng. Data*, **57**, 670 (2012).
50. Z. Yang, A. Soriano, A. Caparanga and M. Li, *J. Chem. Thermodyn*., **42**, 659 (2010).
51. S. Mazinani, A. Samsami, A. Jahanmiri and A. Sardarian, *J. Chem. Eng. Data*, **56**, 3163 (2011).
52. S. Dash and S. Bandyopadhyay, *J. Greenh. Gas Con*., **44**, 227 (2016).
53. H. Lia, Y. Moullec, J. Lu, J. Chen, J. Marcos and G. Chen, *Int. J. Greenh. Gas Con*., **31**, 25 (2014).
54. Y. Kim, J. Choi, S. Nam, S. Jeong and Y. Yoon, *Energy Fuels*, **26**, 1449 (2012).
55. S. Park, H. Song and J. Park, *Fuel Process. Technol*., **120**, 48 (2014).
56. Sh. Shen, X. Feng, R. Zhao, U. Ghosh and A. Chen, *Chem. Eng. J*., **222**, 478 (2013).
57. Ch. Liao and M. Li, *Chem. Eng. Sci*., **57**, 4569 (2002).
58. S. Paul, A. Ghoshal and B. Mandal, *Chem. Eng. Sci*., **64**, 1618 (2009).
59. W. Sun, Ch. Yang and M. Li, *Chem. Eng. Sci*., **60**, 503 (2005).
60. P. Vaidya and E. Kenig, *Chem. Eng. Sci*., **62**, 7344 (2007).
61. Ch. Lin, A. Soriano and M. Li, *J. Taiwan Inst. Chem. E*., **40**, 403 (2009).
62. H. Pawlak, *Int. J. Greenh. Gas Con*., **37**, 76 (2015).
63. A. Rayer, Y. Armugan, A. Henni and P. Tontiwachwuthikul, *J. Chem. Eng. Data*, **59**, 3610 (2014).
64. B. Mondal, S. Bandyopadhyay and A. Samanta, *Fluid Phase Equilib*., **402**, 102 (2015).
65. J. Carson, K. Marsh and A. Mather, *J. Chem. Thermodyn*., **32**, 1285 (2000).
66. J. Lee, F. Otto and A. Mather, *J. Chem. Eng. Data*, **17**, 465 (1972).
67. S. Rho, Y. Lee, J. Nam, S. Son and J. Min, *J. Chem. Eng. Data*, **42**, 1161 (1997).
68. M. Li and K. Shen, *Fluid Phase Equilib*., **85**, 129 (1993).
69. H. Liu, M. Xiao, X. Luo, H. Gao, R. Idem and P. Tontiwachwuthikul, *AIChE J*., **63**, 4465 (2017).
70. R. Zhang, X. Zhang, Q. Yang, H. Yu and X. Luo, *Appl. Energy*, **205**, 1002 (2017).
71. M. Arshad, H. Svendsen, Ph. Fosbol, N. Solms and K. Thomsen, *J. Chem. Eng. Data*, **59**, 764 (2014).
72. H. Li, Y. Moullec, J. Lu, J. Chen, J. Marcos and G. Chen, *Int. J. Greenh. Gas Con*., **31**, 25 (2014).
73. S. Singto, T. Supap, R. Idem, P. Tontiwachwuthikul, S. Tantayanon and M. Almarri, *Sep. Purif. Technol*., **167**, 97 (2016).
74. T. Sema, A. Naami, R. Idem and P. Tontiwachwuthikul, *Ind. Eng. Chem. Res*., **50**, 14008 (2011).
75. M. Majchrowicz and D. Brilman, *Chem. Eng. Sci*., **72**, 35 (2012).
76. X. Chen and G. Rochelle, *Ind. Eng. Chem. Res*., **52**, 4229 (2013).
77. F. Chowdhury, H. Okabe, H. Yamada, M. Onoda and Y. Fujioka, *Energy Procedia*, **4**, 201 (2011).
78. M. Hilliard and Ph.D. Dissertation, The University of Texas at Austin (2008).
79. I. Kim, K. Hoff, E. Hessen, T. Haug-Warberg and H. Svendsen, *Chem. Eng. Sci*., **64**, 2027 (2009).
80. K. Maneeintr, R. Idem, P. Tontiwachwuthikul and A. Wee, *Ind. Eng. Chem. Res*., **49**, 2857 (2010).
81. A. Shariff and M. Shaikh, Energy efficient solvents for CO_2 capture by gas-liquid absorption, Aqueous amino acid salts and their blends as efficient absorbents for CO_2 capture, Springer, 117 (2017).
82. G. Capannelli, A. Comite, C. Costa and R. Di Felice, *Ind. Eng. Chem. Res*., **52**, 13128 (2013).
83. Y. Zhao, Y. Bian, H. Li, H. Guo, Sh. Shen, J. Han and D. Guo, *Energy Fuels*, **31**, 14033 (2017).
84. A. Gomez, A. Jayakumar and N. Mahinpey, *Ind. Eng. Chem. Res*., **55**, 11022 (2016).
85. L-Histidine; MSDS, Science Lab. http://www.sciencelab.com/msds.php?msdsId=9927189.
86. Y. Tada, N. Yano, H. Takahashi, K. Yuzawa, H. Ando, Y. Kubo, A. Nagasawa, K. Chin and Y. Kawamata, *J. Toxicol. Pathol*., **23**, 39 (2010).
87. Glycine; MSDS, Science Lab. http://www.sciencelab.com/msds.php?msdsId=9927179.
88. L-Glutamine, MSDS, Science Lab. http://www.sciencelab.com/msds.php?msdsId=9924160.
89. L-Alanine, http://www.cdhfinechemical.com/images/product/msds/132_1508466045_L-Alanine-CASNO-56-41-7-MSDS.pdf.
90. L-proline, MSDS, Science Lab. http://www.sciencelab.com/msds.php?msdsId=9927237.
91. Taurine, MSDS, Science Lab. http://www.sciencelab.com/msds.php?msdsId=9925166.
92. https://pubchem.ncbi.nlm.nih.gov/compound/2-_2-Aminoethylamino_ethanol#section=Top.
93. https://www.caymanchem.com/msdss/700517m.pdf.
94. Triethanolamine, MSDS, Science Lab. http://www.sciencelab.com/msds.php?msdsId=9927306.
95. http://www.sciencelab.com/msds.php?msdsId=9922894.

96. 2-Methylpiperazine https://www.fishersci.com/.
97. 2-(1-Piperazinyl)-ethylamine, http://www.merckmillipore.com/.
98. Diethanolamine; MSDS, Science Lab.http://www.sciencelab.com/msds.php?msdsId=9923743.
99. Monoethanolamine; MSDS, Science Lab. http://www.sciencelab.com/msds.php?msdsId=9922885.
100. Piperazine; MSDS Science Lab. http://www.sciencelab.com/msds.php?msdsId=9926575.
101. M. Majchrowicz, S. Kersten and W. Brilman, *Ind. Eng. Chem. Res*., **53**, 11460 (2014).
102. Sh. Shen, Y. Yang, Y. Wang, Sh. Ren, J. Han and A. Chen, *Fluid Phase Equilib*., **399**, 40 (2015).